Research Article

Qingwen Shi#, Jiaqi Zou#, Chen Pan, Yin Fu, Mahfzun Nahar Supty, Jiuxiao Sun*, Chunlong Yi, Jingchuan Hu, and Haiying Tan*

Study of the phase-transition behavior of $(AB)_3$ type star polystyrene-*block*-poly(*n*-butylacrylate) copolymers by the combination of rheology and SAXS

https://doi.org/10.1515/epoly-2022-0088
received October 05, 2022; accepted November 07, 2022

Abstract: A series of three-armed star polystyrene-*block*-poly(*n*-butylacrylate) copolymers $(PS\text{-}b\text{-}PBA)_3$ were synthesized to study the phase-transition behavior of the copolymers. The order-to-disorder transition temperature has been determined by oscillatory at different temperatures and dynamic temperature sweep at a fixed frequency. Moreover, the micro-phase separation in the block copolymers has been evaluated by time–temperature superposition, while the free volume and the active energy of the copolymers have been calculated. Interestingly, active energy decreased with the increase in the molecular weight of the PBA components. To further determine the order-to-disorder transition temperature precisely, small angle X-ray scattering was performed at different temperatures. These results confirm that the chain mobility of the star-shaped copolymers is strongly dependent on the arm molecular weight of the star polymers, which will be beneficial for the processing and material preparation of the block copolymers.

Keywords: star block copolymer, phase-transition, polystyrene-*block*-poly(*n*-butylacrylate)

1 Introduction

Block copolymers covalently bonded by chemically distinct repeat units in their molecules have showed special features (1–13). One of their most important features is the melt phase behavior (3,8,14–18). Due to their distinct chemical units, special microphase separation can be detected (3,17,19). For example, formed ordered microdomains with the length scale of the order at distinguished temperature which is comparable to the size of the molecules. This transition of the copolymers is called order–disorder transition (ODT) and the temperature when the transition occurs is called the order–disorder transition temperature (T_{ODT}) (20–24). For linear block copolymers, an order-to-disorder transition can be observed in the block copolymers, which consist of two dissimilar polymer counterparts with favorable segmental interaction between the two components. To our best knowledge, linear block copolymer loses "solid-like" properties in the disordered state, which is well evidenced by a sharp drop in storage modulus (G') (14,25–27). But for star block copolymers, due to the existence of star core which hinders the chain retraction of the branched chain, thus, resulting in their different phase behaviors. Although, some of the star blocks show ODT when increasing the temperature, others undergo a transition from disorder-to-order when heated (e.g., LDOT) (14,21,28–30). However,

# These authors contributed equally to this work.

*** Corresponding author: Jiuxiao Sun,** State Key Laboratory of New Textile Materials and Advanced Processing Technologies, and Key Laboratory of Textile Fiber and Products of Ministry of Education, College of Materials Science and Engineering, Wuhan Textile University, Wuhan, 430200, China, e-mail: 15804638@qq.com
*** Corresponding author: Haiying Tan,** State Key Laboratory of New Textile Materials and Advanced Processing Technologies, and Key Laboratory of Textile Fiber and Products of Ministry of Education, College of Materials Science and Engineering, Wuhan Textile University, Wuhan, 430200, China, e-mail: hytan@wtu.edu.cn
Qingwen Shi, Jiaqi Zou, Chen Pan, Yin Fu, Mahfzun Nahar Supty, Jingchuan Hu: State Key Laboratory of New Textile Materials and Advanced Processing Technologies, and Key Laboratory of Textile Fiber and Products of Ministry of Education, College of Materials Science and Engineering, Wuhan Textile University, Wuhan, 430200, China
Chunlong Yi: China CAMA Engineering Wuhan University Design & Research Company Limited (Camce Whu Design & Research Co., Ltd), Wuhan, 430000, China

the influence of the branched chain on the phase transition behavior is still not very clear.

Buzza et al. studied the ODT of the hetero-four-arm star copolymers (A_2B_2), and found that A_2B_2 have a slightly higher T_{ODT} than that of diblock copolymers with similar segment interaction (16,31). Xu et al. studied the phase behavior of 21-armed star branched polymer in bulk and confinement using the self-consistent mean field theory (32). Based on the stimulation results, they found that star block copolymers showed symmetrical phase diagram in bulk. In addition, the phase boundaries of star block copolymers shift when increasing the arm numbers. Wu et al. studied the influence of the arm number on the phase behavior of star blocks using rheology measurement with the volume fraction of one block fixed at 0.50 (25). With the computer stimulation, they found that the relaxation time of the blocks increased with the arm number, and the phase behavior of the blocks changed from disorder to order when the temperature is increased (17). Regarding the phase behavior, self-consistent field theory simulations have confirmed that the inner blocks of the star copolymers preferentially locate inside of the micro-domains (15). All these studies focus on the influence of the arm numbers and the composition of the star copolymers on the phase behavior of the star blocks. However, the influence of the volume fraction of the block or the molecular weight of the blocks on the phase behavior of the star block copolymers is still not very clear.

In this work, a series of three-armed star polystyrene-*block*-poly(*n*-butylacrylate) copolymers were synthesized. The order-to-disorder transition of the copolymers was investigated by rheology and small angle X-ray scattering (SAXS). Moreover, the influence of the molecular weight on the visco-elastic properties and micro-phase separation was systematically investigated. The (PS-*b*-PBA)$_3$ showed disordered structure at low temperature. The low disorder-to-order transition temperature (T_{LDOT}), the active energy, and free volume changed with the variation of molecular weight of the block copolymers; and the properties of block copolymers will change accordingly, which will be beneficial for preparing and processing the block copolymer materials.

2 Experimental section

2.1 Materials

Copper bromide (CuBr, 99.999%) and 1,3,5-tribromomethylbenzene were purchased from Aldrich. 2,2′-Dipyridyl was purchased from Alladin. Styrene (99%), *n*-butylacrylate (99%), phenyl ether, toluene, *N*,*N*-dimethylformamide (DMF, AR), tetrahydrofuran (THF, AR), dichloromethane, ethanol, and neutral alumina were purchased from China National Medicines Corporation Ltd. Styrene and *n*-butylacrylate were distilled over CaH_2 prior to use. Toluene was purified by Braun system. All the other reagents were used as received.

2.2 Synthesis of three-armed polystyrene (S*x*)$_3$

Three-armed PS was synthesized by atom transfer radical polymerization (ATRP) based on our previous report (33,34). CuBr (0.60 mmol) and 2,2-bipyridyl (Bipy) (1.20 mmol) were added into a dry flask. The flask was sealed with a septum and subsequently purged with dry argon for several minutes. Then, 30 mL of distilled styrene was added with a degassed syringe. The mixture turned dark brown, indicating complexation of CuBr and Bipy. At last, 1,3,5-tribromomethylbenzene (0.60 mmol) was added with a precision syringe. The mixture was heated at 100°C in an oil bath. After 2–12 h, the experiment was stopped by opening the flask and exposing the catalyst to air. The final mixture was diluted with CH_2Cl_2/THF. The solution was filtered through a column filled with neutral alumina to remove the copper complex. After that, the polymer was precipitated in ethanol. Finally, the product was dried at 60°C under vacuum for more than 48 h. ^{1}H NMR ($CDCl_3$) δ (ppm): 7.3–6.3 (m, 5H, aromatic), 4.5 (broad, 1H, CHBr), 2.1–1.0 (m, aliphatic main chain). The obtained samples were named as (**S*x***)$_3$, in which *x* represented the weight-average molecular weight of (**S*x***)$_3$.

2.3 Synthesis of three-armed star polystyrene-*block*-(*n*-butylacrylate) copolymer (S*x*-*b*-B*y*)$_3$

CuBr (0.60 mmol) and 2,2-bipyridyl (Bipy) (1.20 mmol) were added into a dry flask. The flask was sealed with a septum and subsequently purged with dry argon for several minutes. Then, 25 mL of distilled *n*-butylacrylate was added with a degassed syringe. The mixture turned dark brown, indicating the formation of complexation of CuBr and Bipy. Subsequently, a certain content of (**S***x*)$_3$ dissolved in toluene was added with a precision syringe. The mixture was heated to 100°C in an oil bath. After 3 h polymerization, the experiment was stopped by opening

the flask and exposing the catalyst to air. The final mixture was diluted with CH_2Cl_2/THF (1:1) and was then filtered through a column filled with neutral alumina to remove the copper complex. Subsequently, the polymer was precipitated in ethanol, followed by drying at 60°C under vacuum for more than 48 h. The obtained samples are symbolled as (**S***x*-*b*-B*y*)$_3$, in which x and y represents the number-average molecular weight of PS and PBA, respectively. b represents the volume faction of polystyrene (ϕ_{PS}), which is calculated by the following relationship:

$$\phi_{PS} = \frac{M_{w,PS}/\rho_{PS}}{(M_{w,PS-BA} - M_{w,PS})/\rho_{PBA} + M_{w,PS}/\rho_{PS}} \quad (1)$$

where $M_{w,PS-BA}$ and $M_{w,PS}$ are the molecular weight of (PS-PBA)$_3$ and PS chain, respectively. ρ_{PBA} and ρ_{PS} are the density of PS and PBA with the value of 1.05 g·cm^{-3} and 1.08 g·cm^{-1} (26), respectively.

2.4 Characterization

^{1}H NMR spectra were recorded on a Bruker AV 400 MHz spectrometer with $CDCl_3$ as a solvent. Number-average molecular weights (M_n) and polydispersity indices (PDI) were measured by size exclusion chromatography (SEC) coupled to a multi-angle laser light scattering (MALLS) detector (HELEOS, laser wavelength λ = 662 nm), a refractive index detector (Optilab rEX, λ = 658 nm), and a viscosity detector (ViscoStar) (Wyatt Technology). For all SEC analyses, HPLC grade THF was used as the mobile phase at 25°C (flow rate: 1 mL·min^{-1}). The refraction index (d_n/d_c) values were measured by an Optilab T-rEX (Wyatt RI detector, LED light 658.0 nm) through six different concentrations of polymer solution with a flow rate of 1 mL·min^{-1}. Data acquisition was performed using Wyatt Technology WinAstra6 software. M_n, PDI, d_n/d_c, and R_g of star copolymers are summarized in Table 1, as well as the molecular weight of the arm (M_a) of (PS-*b*-PBA)$_3$. Differential scanning calorimeter (DSC, Mettler-Toledo DSC 1) measurement, calibrated with an indium standard, was performed with a sample mass of 5–10 mg. Dry N_2 was passed (95–100 mL·min^{-1}) through the DSC cell during measurement. The block copolymers were heated from room temperature to 200°C at a rate of 10°C·min^{-1}, followed by holding at 200°C for 5 min to erase the thermal history. Then, the samples were cooled to −100°C at a rate of 10°C·min^{-1}. The samples were then reheated to 200°C at a rate of 10°C·min^{-1} (e.g., second heat). Data associated with the glass transition were extracted from the second heat scan. The rheological experiments of the samples were performed on a strain-controlled rheometer (ARES-G2, TA Instruments) using a parallel plate geometry (diameter: 25 mm). Temperature was controlled by a forced convection oven unit under a nitrogen gas purge to minimize the degradation of the samples. Strain amplitude sweep at a fixed frequency (ω = 1 rad·s^{-1}) was performed to establish the linear viscoelastic regime. Oscillatory frequency sweeps were performed from 0.1 to 200 rad·s^{-1} with a strain in the linear regime at various temperatures (110–200°C). Temperature ramp was performed at a fixed frequency of 0.25 rad·s^{-1}. To prevent the degradation of the polymers, all the measurements were performed under N_2 atmosphere. SAXS was performed on a Xeuss 2.0 system of Xenocs France equipped with a semiconductor detector (Pilatus3R 1M, DECTRIS, Swiss) and the X-ray source is MetalJet-D2 (Excillum, Sweden). The wavelength of the X-ray is 0.134 nm. All the measurements were performed at different temperatures ranging from 30°C to 160°C with the temperature interval at 2.5°C. All the measurements were performed without changing the detection place.

Table 1: Molecular structure parameters of the (**S***x*)$_3$ and the star block copolymer (**S***x*-*b*-B*y*)$_3$

Sample	M_n[a] (kDa)	M_w (kDa)	d_n/d_c	$M_{n,PBA}$[b] (kDa)	PDI	R_g (nm)	ϕ_{PBA}[c]
(**S***15.4*)$_3$	46.3	49.9	0.1814	0.0	1.08	5.6	0.00
(**S***15.4-0.94*-**B***1.4*)$_3$	50.6	52.9	0.1760	4.3	1.05	6.3	0.06
(**S***15.4-0.48*-**B***16.7*)$_3$	96.3	103.9	0.1213	50.0	1.08	8.6	0.52
(**S***15.4-0.28*-**B***34.3*)$_3$	149.0	182.0	0.1034	102.7	1.22	11.8	0.72
(**S***15.4-0.21*-**B***46.6*)$_3$	186.0	241.0	0.0839	139.7	1.29	12.6	0.79

[a]Determined by SEC-MALLS in THF at 25°C. [b]Calculated by the relationship as follows: $M_{n,PBA} = M_{n,SPS-BA} - M_{n,SPS}$, [c]Calculated through Eq. 1.

3 Results and discussion

3.1 Synthesis of three-arm star polystyrene-*block*-(*n*-butylacrylate) copolymer (S*x*-*b*-B*y*)$_3$

In this study, a series of three-armed star polystyrene-*block*-(*n*-butylacrylate) copolymers were synthesized using bromo-terminated (**S***x*)$_3$ as the macromolecular initiator via ATRP polymerization. Scheme 1 illustrates the synthesis procedure for the star block copolymer. The molecular weight of the block copolymers was determined by SEC-MALLS, which is given in Table 1. Figure A1 shows the typical ^{1}H NMR spectrum of (**S***x*-*b*-**B***y*)$_3$. The peak at 7.3–6.3 ppm can be ascribed to the protons in the aromatic of the block copolymer, while the peaks at 4.03, 2.28, and 1.90–0.94 ppm can be ascribed to the protons in –OCH$_2$, (–C═O)–CH–, and the aliphatic main chain in (**S***x*-*b*-**B***y*)$_3$, respectively.

3.2 Thermal properties

Figure 1 shows the DSC results measured at the heating rate of 10°C·min^{-1} from –100°C to 200°C. The DSC curves were obtained during the second heating run to eliminate the thermal history, while the glass transition temperature (T_g) estimated from the curves is summarized in Table 2. T_g of three-armed star polystyrene (**S***15.4*)$_3$ was 103.4°C, while it is 71.6°C for (**S***15.4-0.94*-**B***1.4*)$_3$. The copolymer (**S***15.4-0.94*-**B***1.4*)$_3$ showed a single thermal transition peak, like the homogenous polymer (**S***15.4*)$_3$, indicating that no phase separation appears in the block of the polymer. In contrast, (**S***15.4-0.48*-**B***16.7*)$_3$ showed double T_gs peaks at –41.9°C and 84.2°C. Similarly, double T_gs peaks (at –43.2°C and 85.8°C, respectively) appears when the volume fraction of PBA raises to 72% (**S***15.4-0.28*-**B***34.3*)$_3$. The two separated T_gs indicated a pronounced micro-phase separation due to the immiscibility of PS and PBA (14). However, single T_g (at –45.5°C, close to T_g of PBA homopolymer) appears again with the

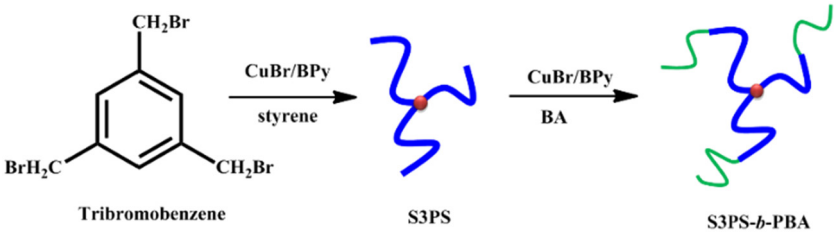

Scheme 1: Schematically shows the synthesis procedure of three-arm star polystyrene-*block*-(*n*-butylacrylate) copolymer.

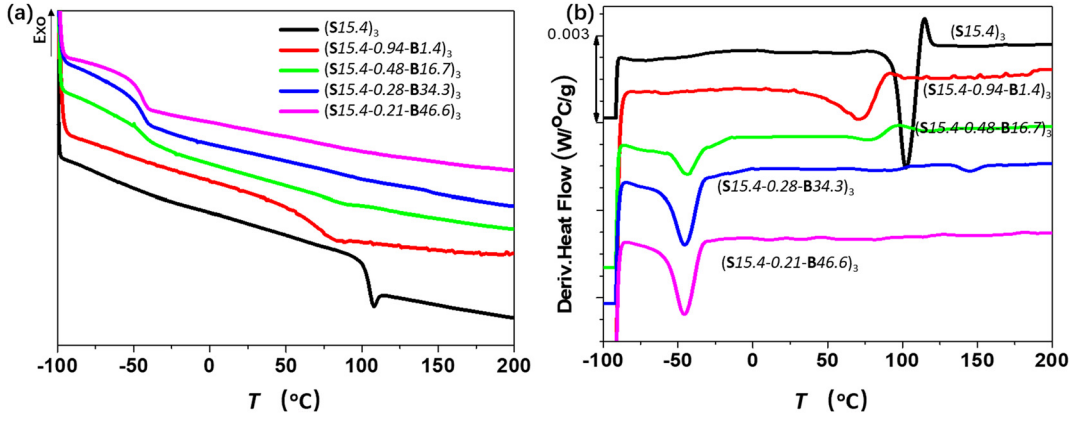

Figure 1: DSC curves for all the synthesized copolymers: **S***46*, (**S***15.4-0.94*-**B***1.4*)$_3$, (**S***15.4-0.48*-**B***16.7*)$_3$, (**S.***4-0.28*-**B.***3*)$_3$, and (**S.***4-0.21*-**B***46.6*)$_3$. (a) Heat flow of the synthesized polymer and (b) differential of the heat flow versus temperature for all the block copolymers. These curves were obtained during the second heating run.

Table 2: Glass transition temperature (T_g) of the block copolymers

Sample	T_g (°C)			Delta C_p
	Onset	Offset	Midpoint	
$(\mathbf{S}15.4)_3$	101.4	105.7	103.4	0.268
$(\mathbf{S}15.4\text{-}0.94\text{-}\mathbf{B}1.4)_3$	69.8	76.4	71.6	0.140
$(\mathbf{S}15.4\text{-}0.48\text{-}\mathbf{B}16.7)_3$	−49.9	−41.8	−41.9	0.171
	70.2	87.8	84.2	0.083
$(\mathbf{S}15.4\text{-}0.28\text{-}\mathbf{B}34.3)_3$	−49.7	−38.1	−43.2	0.277
	72.3	89.2	85.8	0.075
$(\mathbf{S}15.4\text{-}0.21\text{-}\mathbf{B}46.6)_3$	−50.8	−40.4	−45.5	0.238

PBA fraction increasing to 79% when the arm molecular weight of the star block copolymer reaches 62 kg·mol^{-1}.

3.3 Rheology measurement

Dynamic rheological measurement is an efficient way to determine the order-to-disorder transition temperature (T_{ODT} or T_{LDOT}) of the block copolymers, thanks to the sensitivity of the rheology in viscoelastic response of different micro-phases. T_{ODT} (or T_{LDOT}) can be determined accordingly from a significant increase in the storage modulus (G') at a certain temperature (8,14,16,25,35). The dynamic modulus including G' and loss modulus (G'') at different temperatures were measured. Besides, the dynamic temperature sweeps were carried out as well at a fixed frequency of 1 rad·s^{-1} and strain of 1% within the linear viscoelastic region. Figure A2 shows G', G'', and complex viscosity ($|\eta^*|$) versus angular frequency for $(\mathbf{S}15.4)_3$ and $(\mathbf{S}15.4\text{-}0.94\text{-}\mathbf{B}1.4)_3$. No clear difference can be seen in G' and G'' for both $(\mathbf{S}15.4)_3$ and $(\mathbf{S}15.4\text{-}0.94\text{-}\mathbf{B}1.4)_3$, suggesting that no aggregates or phase separation appear during the measurement. Thus, the active energy and free volume of these two polymers were determined. For the homogeneous polymer and copolymer with temperature far above the T_{ODT}, G' and G'' can be constructed via time–temperature superposition (TTS) (16,36–39). The G' and G'' at different temperatures were shifted horizontally along the x-axis with respect to a reference temperature (T_{ref} = 150°C), and the shift factor was independently calculated to ensure the best overlap between the adjacent isotherms. The shifted curves were expressed by the following equation:

$$G^{\#}(T, a_T w) = G^{\#}(T_{ref}, w) \tag{2}$$

where T and T_{ref} represent the measuring temperature and reference temperature, respectively. $G^{\#}$ represents G' or G'', ω is the angular frequency, and α_T is the horizontal shift factor. The G' and G'' of $(\mathbf{S}15.4)_3$ and $(\mathbf{S}15.4\text{-}0.94\text{-}\mathbf{B}1.4)_3$ obey TTS principle, suggesting that the sample is homogeneous within the measuring range. This is coincidence with the DSC results that both samples appear as single T_g. Comparing the G' and G'' of $(\mathbf{S}15.4\text{-}0.94\text{-}\mathbf{B}1.4)_3$ with $(\mathbf{S}15.4)_3$, the lower modulus of copolymer can be observed at the same temperature, which can be ascribed to the soft PBA chains in the block copolymer $(\mathbf{S}15.4\text{-}0.94\text{-}\mathbf{B}1.4)_3$. Moreover, shift factor can be determined (Figure A2c and e) according to TTS principle. The relationship between shift factor and temperature can be depicted by Arrhenius (Eq. 3) (40) and Williams–Landel–Ferry (41,42) (WLF, Eq. 4) relationship:

$$\lg(\alpha_T) = \frac{E_a}{R}\left(\frac{1}{T} - \frac{1}{T_{ref}}\right) \tag{3}$$

where α_T represents the horizontal shift factor, T and T_{ref} are the measuring temperature and reference temperature, respectively, and E_a is the active energy. WLF equation can be written as follows:v

$$\lg(\alpha_T) = -\frac{C_1^g(T - T_g)}{C_2^g + (T - T_g)} \tag{4}$$

where $C_1^g = B/2.303f_g$ and $C_2^g = f_g/\alpha_f$, α_T represents the horizontal shift factor, T and T_g represent the measuring temperature and glass transition temperature, respectively, f_g is the fractional free volume at T_g, α_f is the temperature coefficient of fractional free volume, and B is a constant.

Table 3: Viscoelastic properties of all the $(PS\text{-}b\text{-}PBA)_3$ samples at T_{ref} = 150°C determined from rheology measurement based on Arrhenius and WLF relationship

Sample	C_1	C_2	E_a	f_g/B	f_{ref}/B	$\alpha_f/B\times10^{-4}$
$(\mathbf{S}15.4)_3$	6.82	112.25	175.75	0.0372	0.0637	5.67
$(\mathbf{S}15.4\text{-}0.94\text{-}\mathbf{B}1.4)_3$	3.77	114.78	116.02	0.0413	0.115	10.03
$(\mathbf{S}15.4\text{-}0.48\text{-}\mathbf{B}16.7)_3$	2.86	107.11	95.35	—	—	—
$(\mathbf{S}15.4\text{-}0.28\text{-}\mathbf{B}34.3)_3$	3.32	174.01	74.72	—	—	—
$(\mathbf{S}15.4\text{-}0.21\text{-}\mathbf{B}46.6)_3$	2.16	212.83	33.83	0.0206	0.200	9.42

When T_{ref} is different from T_g, Eq. 4 can be rewritten as follows:

$$\lg(\alpha_T) = -\frac{C_1^{ref}(T - T_{ref})}{C_2^{ref} + (T - T_{ref})} \quad (5)$$

where $C_1^{ref} = B/2.303f_{ref}$, $C_1^{ref} = f_{ref}/\alpha_f$ and f_{ref} is the fractional free volume at T_{ref}. α_f is the temperature coefficient of fractional free volume, and B is a constant. From Eqs. 3 and 4, the active energy and free volume can be calculated and summarized as in Table 3. According to the

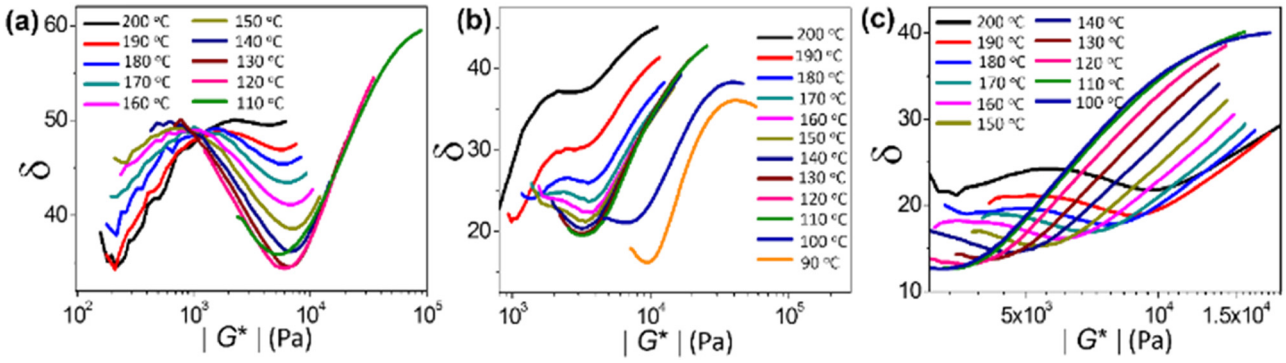

Figure 2: Corresponding vGP plot of phase angle (δ) versus complex modulus ($|G^*|$) of (a) (**S***15.4-0.48*-**B***16.7*)$_3$, (b) (**S***15.4-0.28*-**B***34.3*)$_3$, and (c) (**S***15.4-0.21*-**B***46.6*)$_3$.

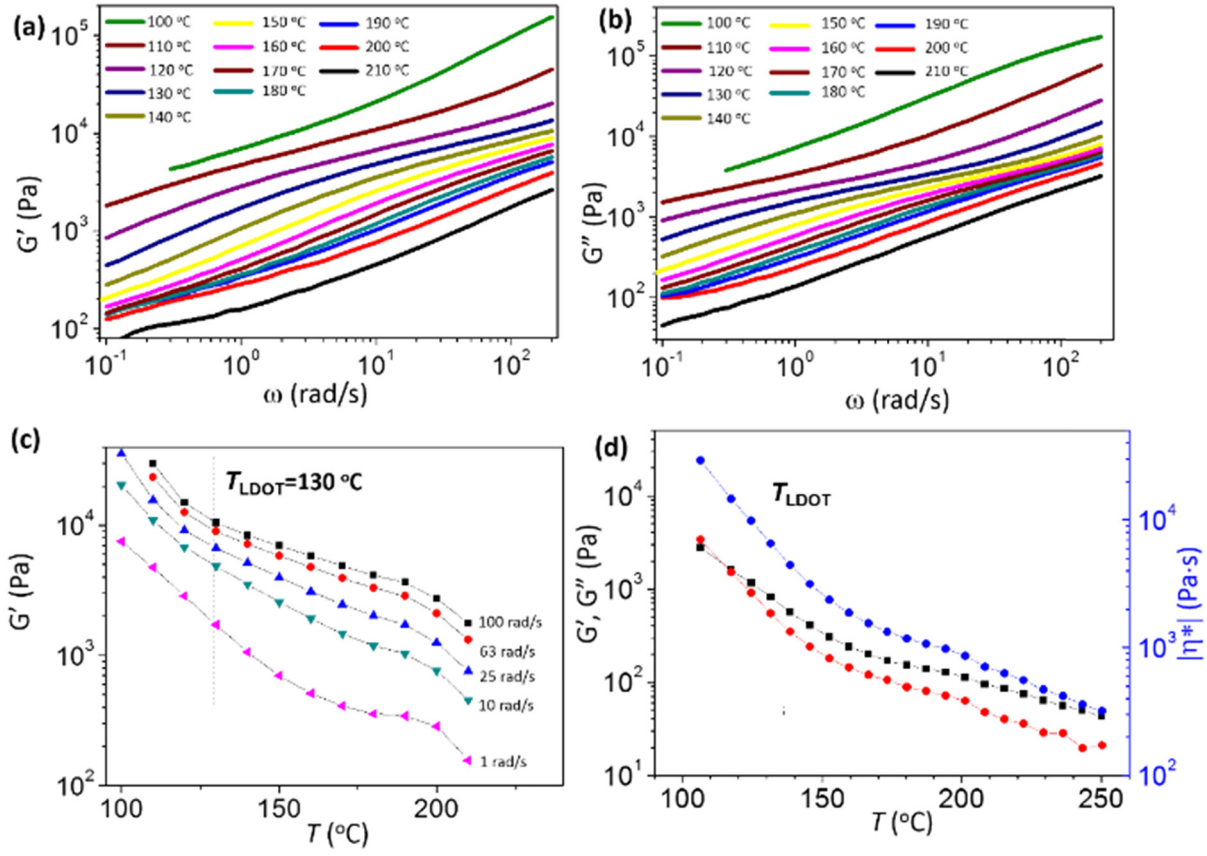

Figure 3: (a) Storage modulus (G') and (b) loss modulus (G'') versus angular frequency (ω) from dynamic oscillation at a fixed temperature range from 100°C to 210°C with the interval of temperature at 1°C for (**S***15.4-0.48*-**B***16.7*)$_3$, (c) isochronal plots of G' versus temperature (T) for (**S***15.4-0.48*-**B***16.7*)$_3$, (d) temperature dependence of the storage modulus (G'), loss modulus (G''), and complex viscosity ($|\eta^*|$) obtained at the strain amplitude 1% and a signal angular frequency 1 rad·s^{-1} during the cooling of (**S***15.4-0.48*-**B***16.7*)$_3$.

WLF theory, we can obtain that $f_{ref} = f_{ref} + \alpha_f (T_{ref} - T_g)$. Based on the relationship in the latter part, the free volume at T_{ref} and T_g can be calculated through the relationships given below:

$$C_1^g = C_1^{ref} C_2^{ref} / (C_1^{ref} + T_g - T_{ref}) \quad (6)$$

$$C_2^g = C_2^{ref} + T_g - T_{ref} \quad (7)$$

$$f_g = B(C_2^{ref} + T_g - T_{ref}) / (2.303 C_1^{ref} C_2^{ref}) \quad (8)$$

Thus, after introducing the PBA chains, active energy of the copolymers is significantly reduced to 175.75 kJ·mol^{-1} for (**S***15.4*)$_3$ and 116.02 kJ·mol^{-1} for (**S***15.4-0.94*-**B***1.4*)$_3$, while the free volume strongly increased from 0.0637 (for **S***15.4*)$_3$ to 0.115 (for **S***15.4-0.94*-**B***1.4*)$_3$. All these results confirm that the incorporation of PBA increases the mobility of polymer chains.

The phase angle (δ) versus complex modulus ($|G^*|$) in van Gurp-Plamen (vGP) (24) at different temperatures are plotted in Figure 2. The plot for (**S***15.4-0.48*-**B***16.7*)$_3$ exhibits a maxima δ peak and clear superposition behavior (at lower temperature $|G^*|$ obey TTS principles) at higher value of $|G^*|$, while it shows less value at lower value of $|G^*|$, which are hypothesized to arise from gradual alignment of the block copolymer domains. This confirms that the star block copolymers show lower disorder-to-order transition (LODT). For (**S***15.4-0.28*-**B***34.3*)$_3$, a transition of δ can be seen at the temperature ranging from 110°C to 130°C (Figure 2), which indicates a transition from disorder to order at this temperature range. Similarly, for (**S***15.4-0.21*-**B***46.6*)$_3$, a transition from disorder to order can be seen at the temperature ranging from 100°C to 110°C. These results confirmed that the transition temperature decreases with the increase of PBA volume fraction.

To further investigate the LDOT behavior of (PS-*b*-PBA)$_3$, rheology measurement was performed by dynamic oscillation at different temperatures. As shown in Figure 3, **S**(**S***15.4-0.48*-**B***16.7*)$_3$ with higher volume fraction of PBA, both G' and G'' showed weaker dependence on angular frequency (ω) when the temperature was higher than 200°C (Figure 3). An abrupt change in G' and G'' can

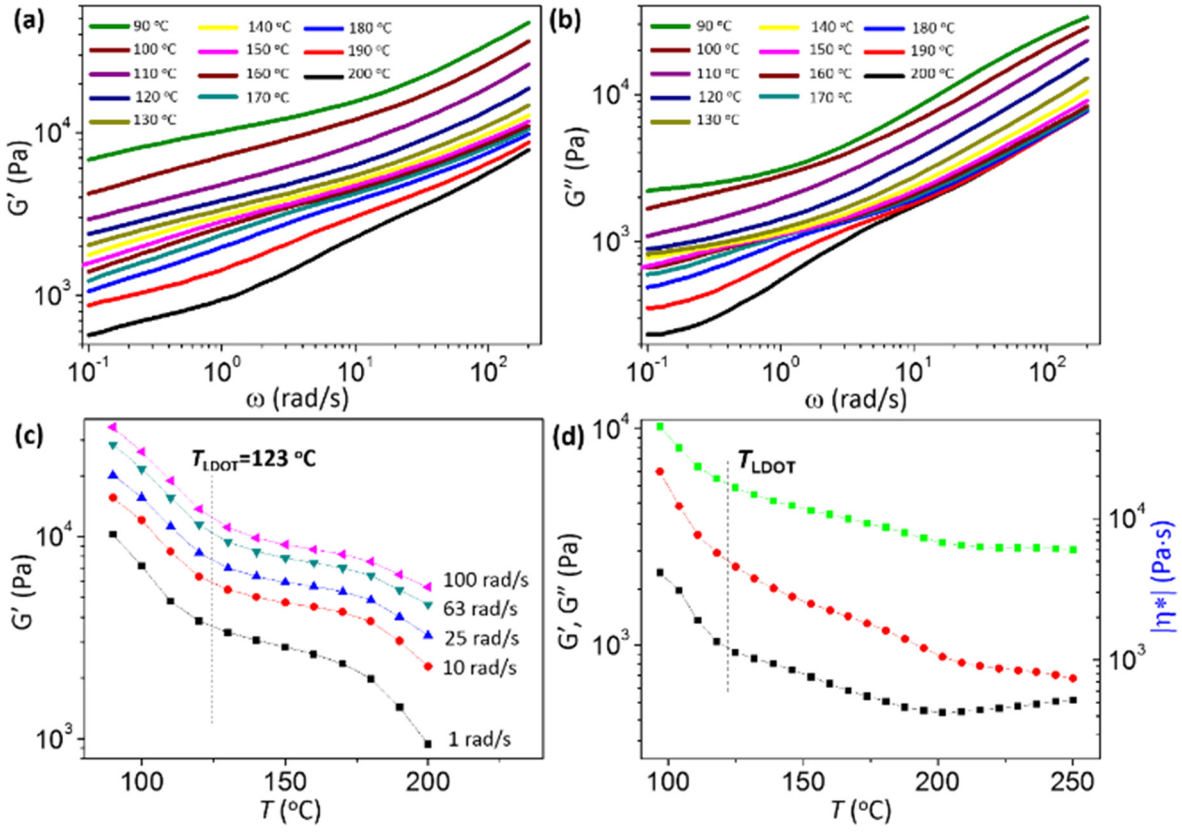

Figure 4: (a) Storage modulus (G') and (b) loss modulus (G'') versus angular frequency (ω) from dynamic oscillation at a fixed temperature range from 100°C to 210°C with the interval of temperature at 10°C for (**S***15.4-0.28*-**B***34.3*)$_3$, (c) isochronal plots of G' versus temperature (T) for (**S***15.4-0.28*-**B***34.3*)$_3$, (d) temperature dependence of the storage modulus (G'), loss modulus (G''), and complex viscosity ($|\eta^*|$) obtained at the strain amplitude 1% and a signal angular frequency 1 rad·s^{-1} during the cooling of (**S***15.4-0.28*-**B***34.3*)$_3$.

be seen, which identifies the ODT (35,43). T_{LDOT} can be determined based on the changing trend of G' at the fixed ω versus T (Figure 3c). Meanwhile, T_{LDOT} can also be estimated from isochronal plot of G' versus T (Figure 3d).

It should be noted that T_{LDOT} of (**S***15.4-0.48*-**B***16.7*)$_3$ obtained by these two ways are nearly the same (T_{LDOT} = 130°C). Besides, the G' and G'' of (**S***15.4-0.48*-**B***16.7*)$_3$ display slightly out of the fitting by the TTS principle (Figure A3), which could be ascribed to the phase separation in this sample. The shift factor can also be determined with the same method as (**S***15.4*)$_3$. The active energy is calculated to be 95.35 kJ·mol^{-1}, which is lower than that of both (**S***15.4*)$_3$ and (**S***15.4-0.94*-**B***1.4*)$_3$. This result indicates that the mobility of (**S***15.4-0.48*-**B***16.7*)$_3$ increases when concentration of PBA chains increases. Unfortunately, the free volume (**S***15.4-0.48*-**B***16.7*)$_3$ cannot be determined due to the existence of two T_gs. Additionally, T_{LDOT} drops significantly with the PBA concentration rising to 0.72 (123°C) and 0.79 (110°C), which is consistent with the DSC results that the T_g drops with the increase in PBA concentration. Similar to the copolymer (**S***15.4-0.48*-**B***16.7*)$_3$, G' and G'' of (**S***15.4-0.28*-**B***34.3*)$_3$ and (**S***15.4-0.21*-**B***46.6*)$_3$ are out of the TTS principle (Figures 4 and 5, Figures A4 and A5).

The T_{LDOT} was 123°C and 110°C. The results by dynamic measurement and temperature sweeps are coincident with each other. T_{LDOT} decreased with the increase of the volume fraction of PBA. Fortunately, the active energy still can be roughly estimated, which is 74.72 kJ·mol^{-1} for (**S***15.4-0.28*-**B***34.3*)$_3$ and 33.83 kJ·mol^{-1} for (**S***15.4-0.21*-**B***46.6*)$_3$. It can be clearly seen that the active energy decreases with the increase of PBA concentration, indicating that the mobility of the polymer chains increased with the increase of PBA concentration. Notably, E_a decreases as well when M_n increases for (PS-*b*-PBA)$_3$ (Figure A6). It seems that this result contradicts the general concept that high molecular weight reduces the mobility of the molecular chains due to the high entanglement of the polymer chains (32,33). The reason can be ascribed to that the mobility of the copolymer chains is more sensitive to the concentration of the component with high mobility, which can be further confirmed by the abrupt decrease in E_a when small molecular weight PBA chain was grafted on the end of PS chain end.

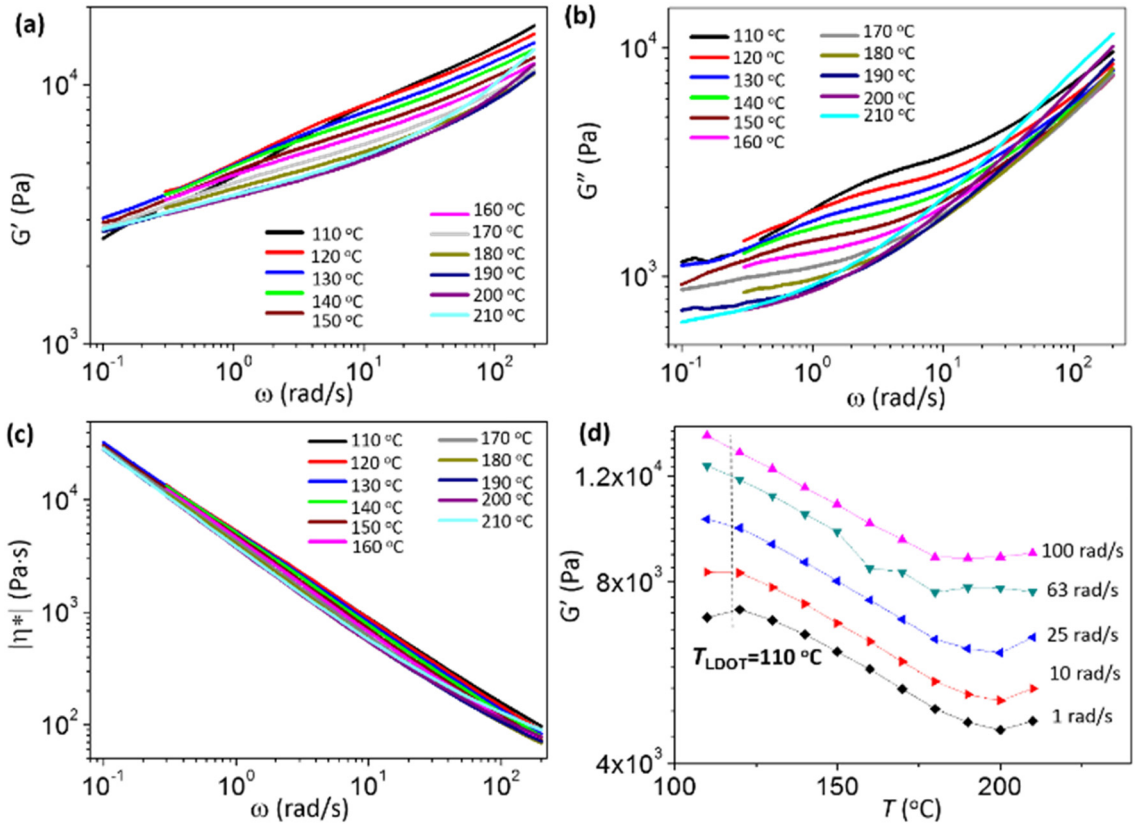

Figure 5: (a) Storage modulus (G'), (b) loss modulus (G''), and (c) complex viscosity ($|\eta^*|$) versus angular frequency (ω) from dynamic oscillation at a fixed temperature range from 100°C to 210°C with the interval of temperature at 10°C for (**S***15.4-0.21*-**B***46.6*)$_3$, and (d) isochronal plots of G' versus temperature (T) for (**S***15.4-0.21*-**B***46.6*)$_3$.

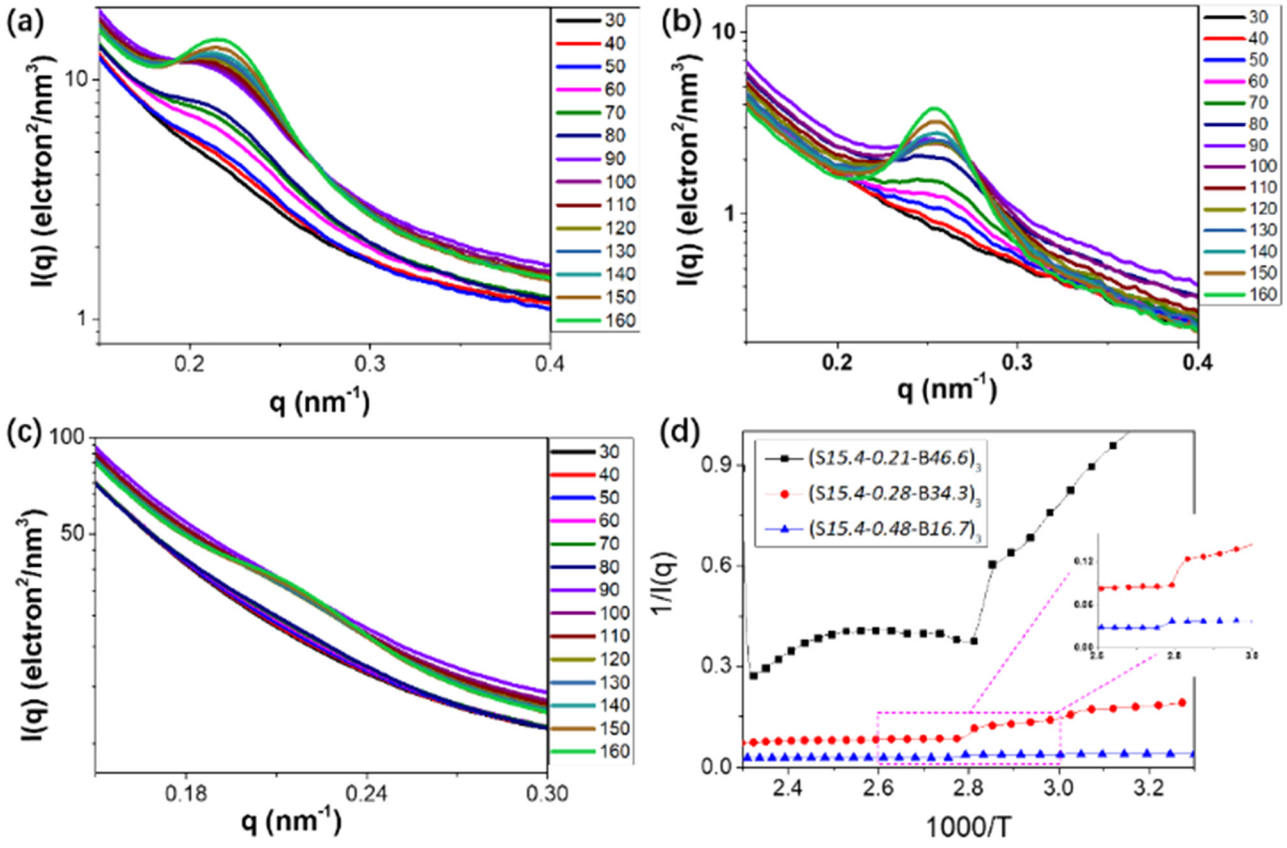

Figure 6: SAXS intensity profiles for the three-armed star block copolymers: (a) (**S***15.4-0.48*-**B***16.7*)$_3$, (b) (**S***15.4-0.28*-**B***34.3*)$_3$, and (c) (**S***15.4-0.21*-**B.***6*)$_3$ at different detection temperatures (from 30°C to 160°C). (d) Inverse of the maximum intensity ($1/I(q^*)$) at the peak position as a function of the inverse temperature (1,000/K) for (**S***15.4-0.48*-**B.***7*)$_3$, (**S***15.4-0.28*-**B***34.3*)$_3$, and (**S***15.4-0.21*-**B***46.6*)$_3$.

3.4 SAXS

From rheology measurement we know that block copolymer showed phase transition behavior when the volume fraction of PS decreased to 0.48 and even lower. The transition temperature for (**S***15.4-0.48*-**B***16.7*)$_3$, (**S***15.4-0.28*-**B***34.3*)$_3$, and (**S***15.4-0.21*-**B***46.6*)$_3$ determined by rheology was 130°C, 123°C, and 110°C, respectively. But from rheology we cannot know whether the ordered structure is formed or not, but the T_{ODT} determined from rheology is not so accurate. Thus, SAXS was performed from 30°C to 150°C to study the phase transition of the block copolymer carefully. Figure 6a–c shows the SAXS spectra of the block copolymers at different temperatures. The intensity profiles were obtained from 30°C to 160°C with the temperature interval at 5°C. When volume fraction of PS was at 48%, at lower temperatures (T < 217°C) intensity weakens and broadens into a broad maximum with the increase in temperature, indicating a transition from an ordered to a disordered state. To our best knowledge, density of SAXS for block polymer is dominated by the scattering concentration fluctuations (44–46). The maximum intensity of the scattering peak for (**S***15.4-0.48*-**B***16.7*)$_3$, (**S***15.4-0.28*-**B***34.3*)$_3$, and (**S***15.4-0.21*-**B***46.6*)$_3$ versus temperature is given in Figure 6a–c. From the abrupt change in 1/I(q) (Figure 6d), we can determine the phase transition temperature of the star blocks. Phase transition temperature for (**S***15.4-0.48*-**B***16.7*)$_3$, (**S***15.4-0.28*-**B***34.3*)$_3$, and (**S***15.4-0.21*-**B***46.6*)$_3$ is 87.6°C, 82.9°C, and 80.9°C, respectively. With the increase in temperature, the star blocks showed ordered structure. The results of SAXS further verified the disorder-to order transition of the star block copolymer PS-*b*-PBA. Except for the phase transition temperature, the main phase of the block copolymer can also be determined. The main phase in the block copolymer was spheres because only one broad peak can be observed.

4 Conclusions

In summary, a series of three-armed star polystyrene-*block*-poly(*n*-butylacrylate) copolymers (PS-*b*-PBA)$_3$ were

synthesized by using ATRP. The (PS-*b*-PBA)$_3$ showed disordered structure at low temperature. The T_{ODT} was determined by oscillatory and dynamic temperature sweep, which decreases with the increase of the volume fraction of poly(*n*-butylacrylate) (PBA) chain. When the volume fraction of PBA chain was small (<0.48), G' and G'' of the block copolymers obey TTS principle. With the increase in the content of PBA, TTS principle failed to explain our result due to the existence of the phase separation as the polymer melts. Moreover, the active energy and free volume was calculated based on Arrhenius and WLF relationship. The active energy decreased with the molecular weight of the block copolymers, while the free volume of the sample increased due to the incorporation of PBA chain, which can strongly enhance the chain mobility of the block copolymers. The disorder-to-order transition temperature of star block PS-*b*-PBA was further determined by SAXS. Phase transition temperature for (**S***15.4-0.48*-**B***16.7*)$_3$, (**S***15.4-0.28*-**B***34.3*)$_3$, and (**S***15.4-0.21*-**B***46.6*)$_3$ is 87.6°C, 82.9°C, and 80.9°C, respectively. With the increase in temperature, the star blocks showed ordered structure.

Funding information: This work was financially supported by the National Natural Science Foundation of China (51803066) and Foundation of HuBei Educational Committee (Q20201710). Thanks for the support from the Open Research Fund of State Key Laboratory of Polymer Physics and Chemistry, Changchun Institute of Applied Chemistry, Chinese Academy of Sciences (2020-18), Open Research Fund of State Key Laboratory of New Textile Materials and Advanced Processing Technologies, Wuhan Textile University (2020-12), and Key Laboratory of Optoelectronic Chemical Materials and Devices of Ministry of Education, Jianghan University (JDGD-202024).

Author contributions: Qingwen Shi and Jiaqi Zou did the experiments and prepared the manuscript; Chen Pan and Yin Fu drew the figures; Mahfzun Nahar Supty and Jingchuan Hu did the temperature sweep experiments; Haiying Tan, Chunlong Yi, and Jiuxiao Sun got the financial support and revised the manuscript.

Conflict of interest: Authors state no conflict of interest.

References

(1) Zhong ZX, Peng L, Zhang N, Su JX, Ye NB, Luo ZF, et al. Miscibility of isotactic polypropylene with random and block ethylene–octene copolymers studied by atomic force microscopy-infrared. Polymer. 2022;259:125345. doi: 10.1016/j.polymer.2022.125354.

(2) Yan N, Liu X, Zhu J, Zhu Y, Jiang W. Well-ordered inorganic nanoparticle arrays directed by block copolymer nanosheets. ACS Nano. 2019;13(6):6638–46. doi: 10.1021/acsnano.9b00940.

(3) Wen T, Wang HF, Georgopanos P, Avgeropoulo A, Ho RM. Three-dimensional visualization of phase transition in polystyrene-block-polydimethylsiloxane thin film. Polymer. 2019;167:209–14. doi: 10.1016/j.polymer.2019.01.047.

(4) Song DP, Zhao THH, Guidetti G, Vignolini S, Parker RM. Hierarchical photonic pigments via the confined self-assembly of bottlebrush block copolymers. ACS Nano. 2019;13(2):1764–71. doi: 10.1021/acsnano.8b07845.

(5) Lee J, Ku KH, Park CH, Lee YJ, Yun H, Kim BJ. Shape and color switchable block copolymer particles by temperature and pH dual responses. ACS Nano. 2019;13(4):4230–7. doi: 10.1021/acsnano.8b09276.

(6) Yang Y, Kim H, Xu J, Hwang MS, Tian D, Wang K, et al. Responsive block copolymer photonic microspheres. Adv Mater. 2018;30(21):1707344. doi: 10.1002/adma.201707344.

(7) Rüttiger C, Hübner H, Schöttner S, Winter T, Cherkashinin G, Kuttich B, et al. Metallopolymer-based block copolymers for the preparation of porous and redox-responsive materials. ACS Appl Mater Interfaces. 2018;10(4):4018–30. doi: 10.1021/acsami.7b18014.

(8) Maher MJ, Jones SD, Zografos A, Xu J, Schibur HJ, Bates FS. The order–disorder transition in graft block copolymers. Macromolecules. 2018;51(1):232–41. doi: 10.1021/acs.macromol.7b02262.

(9) Kim K, Schulze MW, Arora A, Lewis RM, Hillmyer MA, Dorfman KD, et al. Thermal processing of diblock copolymer melts mimics metallurgy. Science. 2017;356(6337):520–3. doi: 10.1126/science.aam7212.

(10) Wang M, Timachova K, Olsen BD. Diffusion mechanisms of entangled rod–coil diblock copolymers. Macromolecules. 2013;5694–701. doi: 10.1021/ma400653g.

(11) Xu J, Li J, Yang Y, Wang K, Xu N, Li J, et al. Block copolymer capsules with structure-dependent release behavior. Angew Chem Int Ed. 2016;55(47):14633–7. doi: 10.1002/anie.201607982.

(12) Borah D, Senthamaraikannan R, Rasappa S, Kosmala B, Holmes JD, Morris MA. Swift nanopattern formation of PS-b-PMMA and PS-b-PDMS block copolymer films using a microwave assisted technique. ACS Nano. 2013;7(8):6583–96. doi: 10.1021/nn4035519.

(13) Fielding LA, Hendley Iv CT, Asenath-Smith E, Estroff LA, Armes SP. Rationally designed anionic diblock copolymer worm gels are useful model systems for calcite occlusion studies. Polym Chem. 2019;10(37):5131–41. doi: 10.1039/C9PY00889F.

(14) Wang W, Wang X, Jiang F, Wang Z. Synthesis, order-to-disorder transition, microphase morphology and mechanical properties of BAB triblock copolymer elastomers with hard middle block and soft outer blocks. Polym Chem. 2018;9(22):3067–79. doi: 10.1039/C8PY00375K.

(15) Matsen MW, Schick M. Microphase separation in starblock copolymer melts. Macromolecules. 1994;27(23):6761–7. doi: 10.1021/ma00101a014.

(16) Buzza DMA, Hamley IW, Fzea AH, Moniruzzaman M, Allgaier JB, Young RN, et al. Anomalous difference in the order–disorder transition temperature comparing a symmetric diblock copolymer AB with its hetero-four-arm star analog A2B2. Macromolecules. 1999;32(22):7483–95. doi: 10.1021/ma9904060.
(17) Shao JY, Jiang NF, Zhang HD, Yang YL, Tang P. Target-directed design of phase transition path for complex structures of rod-coil block copolymers. ACS Omega. 2019;4(23):20367–80. doi: 10.1021/acsomega.9b02984.
(18) Takagi H, Sugino Y, Hara S, Yamamoto K, Okamoto S, Shimada S, et al. Small angle X-ray scattering study on phase transition behavior from crystalline-amorphous alternative lamellar structure to gyroid phase of semicrystalline block copolymer polybutadiene-block-poly(epsilon-caprolactone). Kobunshi Ronbunshu. 2010;67(9):521–9. doi: 10.1295/koron.67.521.
(19) Chakrabarti A, Toral R, Gunton JD. Microphase separation in block copolymers. Phys Rev Lett. 1989;63(24):2661–4.
(20) Lin Y, Chen W, Meng L, Wang D, Li L. Recent advances in post-stretching processing of polymer films with in situ synchrotron radiation X-ray scattering. Soft Matter. 2020;16(15):3599–612. doi: 10.1039/c9sm02554e.
(21) Mortensen K, Annaka M. Stretching PEO–PPO type of star block copolymer gels: Rheology and small-angle scattering. ACS Macro Lett. 2018;7(12):1438–42. doi: 10.1021/acsmacrolett.8b00792.
(22) Kim Y, Yong D, Lee W, Jo S, Ahn H, Kim JU, et al. Preferential wetting effects on order-to-disorder transition in polystyrene-b-poly(2-vinylpyridine) films: a reconsideration on thickness dependence. Macromolecules. 2018;51(21):8550–60. doi: 10.1021/acs.macromol.8b01136.
(23) Khandpur AK, Forster S, Bates FS, Hamley IW, Ryan AJ, Bras W, et al. Polyisoprene-polystyrene diblock copolymer phase diagram near the order–disorder transition. Macromolecules. 1995;28(26):8796–806. doi: 10.1021/ma00130a012.
(24) Ryu DY, Jeong U, Lee DH, Kim J, Youn HS, Kim JK. Phase behavior of deuterated polystyrene-block-poly(n-pentyl methacrylate) copolymers. Macromolecules. 2003;36(8):2894–902. doi: 10.1021/ma026002g.
(25) Wu L, Cochran EW, Lodge TP, Bates FS. Consequences of block number on the order–disorder transition and viscoelastic properties of linear (AB)n multiblock copolymers. Macromolecules. 2004;37(9):3360–8. doi: 10.1021/ma035583m.
(26) Shangguan Y, Chen F, Jia E, Lin Y, Hu J, Zheng Q. New insight into time-temperature correlation for polymer relaxations ranging from secondary relaxation to terminal flow: application of a universal and developed WLF equation. Polymers. 2017;9(11):567.
(27) Rudyak VY, Larin DE, Govorun EN. Microphase separation of statistical multiblock copolymers. Macromolecules. 2022;55(21):9345–57. doi: 10.1021/acs.macromol.2c00065.
(28) Konwar DB, Jacob J, Satapathy BK. A comparative study of poly(l-lactide)-block-poly(ϵ-caprolactone) six-armed star diblock copolymers and polylactide/poly(ϵ-caprolactone) blends. Polym Int. 2016;65(9):1107–17. doi: 10.1002/pi.5168.
(29) Park J, Jang S, Kim JK. Morphology and microphase separation of star copolymers. J Polym Sci Part B-Polym Phys. 2015;53(1):1–21. doi: 10.1002/polb.23604.
(30) Ijichi Y, Hashimoto T, Fetters LJ. Order-disorder transition of star-block copolymers. 2. Eff Arm Number Macromol. 1989;22(6):2817–24. doi: 10.1021/ma00196a048.
(31) Buzza DMA, Fzea AH, Allgaier JB, Young RN, Hawkins RJ, Hamley IW, et al. Linear melt rheology and small-angle X-ray scattering of AB diblocks vs A2B2 four arm star block copolymers. Macromolecules. 2000;33(22):8399–414. doi: 10.1021/ma000382t.
(32) Xu Y, Li W, Qiu F, Lin Z. Self-assembly of 21-arm star-like diblock copolymer in bulk and under cylindrical confinement. Nanoscale. 2014;6(12):6844–52. doi: 10.1039/C4NR01275E.
(33) Tan H, Xu D, Wan D, Wang Y, Wang L, Zheng J, et al. Melt viscosity behavior of C-60 containing star polystyrene composites. Soft Matter. 2013;9(27):6282–90. doi: 10.1039/c3sm00103b.
(34) Tan H, Zhang G, Lin Y, Ma L, Tang T. Synthesis of polystyrene-based Y-shaped asymmetric star by the combination of ATRP/RAFT and its thermal and rheological properties. RSC Adv. 2016;6(108):106648–55. doi: 10.1039/C6RA20541K.
(35) Bi L-K, Fetters LJ. Synthesis and properties of block copolymers. 3. polystyrene-polydiene star block copolymers. Macromolecules. 1976;9(5):732–42. doi: 10.1021/ma60053a010.
(36) Peng M, Zheng Q. Application of time-temperature superposition principle to evaluation of scattering intensity evolution in phase separation for PMMA/SAN blends. Chin J Polym Sci. 2000;18(6):565–8.
(37) Jamarani R, Erythropel HC, Burkat D, Nicell JA, Leask RL, Maric M. Rheology of green plasticizer/poly(vinyl chloride) blends via time-temperature superposition. Processes. 2017;5(3):43. doi: 10.3390/pr5030043.
(38) Gupta R, Baldewa B, Joshi YM. Time temperature superposition in soft glassy materials. Soft Matter. 2012;8(15):4171–6. doi: 10.1039/C2SM07071E.
(39) Enns JB, Gillham JK. Time–temperature–transformation (TTT) cure diagram: Modeling the cure behavior of thermosets. J Appl Polym Sci. 1983;28(8):2567–91. doi: 10.1002/app.1983.070280810.
(40) Al-Malah KIM, Abu-Jdayil B, Zaitoun S, Ghzawi AA-M. Application of wlf and arrhenius kinetics to rheology of selected dark-colored honey. J Food Process Eng. 2001;24(5):341–57. doi: 10.1111/j.1745-4530.2001.tb00548.x.
(41) Ferry JD, Rice SA. Viscoelastic properties of polymers. Phys Today. 1962;15(1):76–8.
(42) Lomellini P. Williams–Landel–Ferry versus Arrhenius behaviour: polystyrene melt viscoelasticity revised. Polymer. 1992;33(23):4983–9. doi: 10.1016/0032-3861(92)90049-3.
(43) Almdal K, Bates FS. Order, disorder, and fluctuation effects in an asymmetric poly(ethylene-propylene)-poly(ethylethylene) diblock copolymer. J Chem Phys. 1992;96(12):9122–32. doi: 10.1063/1.462221.
(44) Floudas G, Pispas S, Hadjichristidis N, Pakula T, Erukhimovich I. Microphase separation in star block copolymers of styrene and isoprene. Theory, experiment, and simulation. Macromolecules. 1996;29(11):4142–54. doi: 10.1021/ma951762v.

(45) Zhu H, Lv Y, Shi D, Li Y-G, Miao W-J, Wang Z-B. A synchrotron in situ X-ray study on the multiple melting behaviors of isomorphous poly(3-hydroxybutyrate-co-3-hydroxyvalerate)(P(HB-co-HV)) with middle HV content. Chin J Polym Sci. 2020;38(9):1015–24. doi: 10.1007/s10118-020-2427-5.

(46) Lee C-F, Wang M-R, Lin T-L, Yang C-H, Chen L-J. Dynamic behavior of the structural phase transition of hydrogel formation induced by temperature ramp and addition of ibuprofen. Langmuir. 2020;36(30):8929–38. doi: 10.1021/acs.langmuir.0c01437.

Appendix

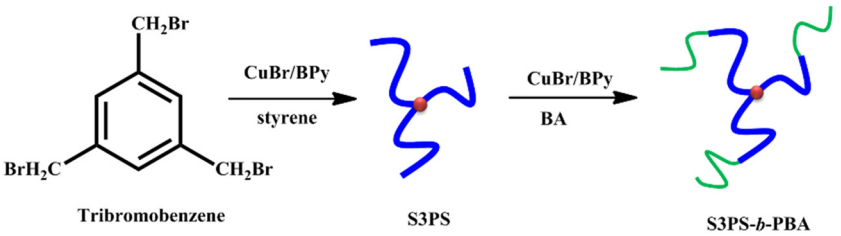

Scheme A1: Illustration showing the procedure for the synthesis of three-arm star polystyrene-*block*-(*n*-butylacrylate) copolymer.

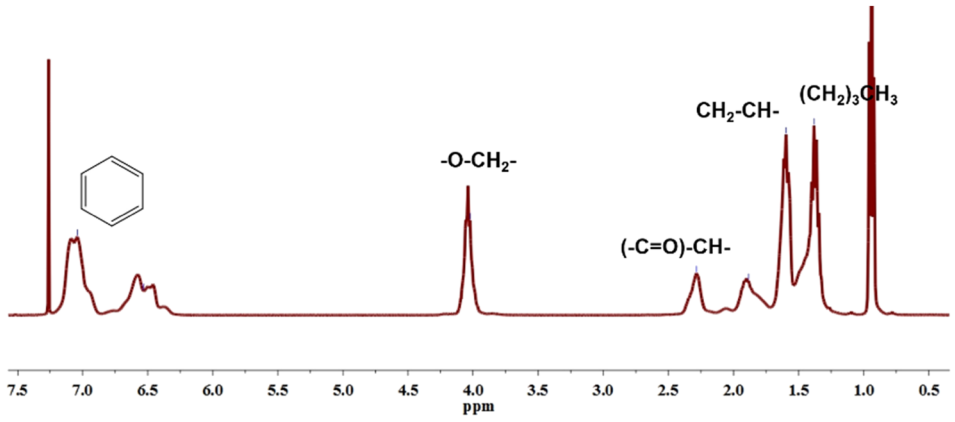

Figure A1: ^{1}H NMR of the synthesized three-arm star polystyrene-*block*-(*n*-butylacrylate) copolymer (**S***x*-*b*-B*y*)$_3$ with $CDCl_3$ as the solvent.

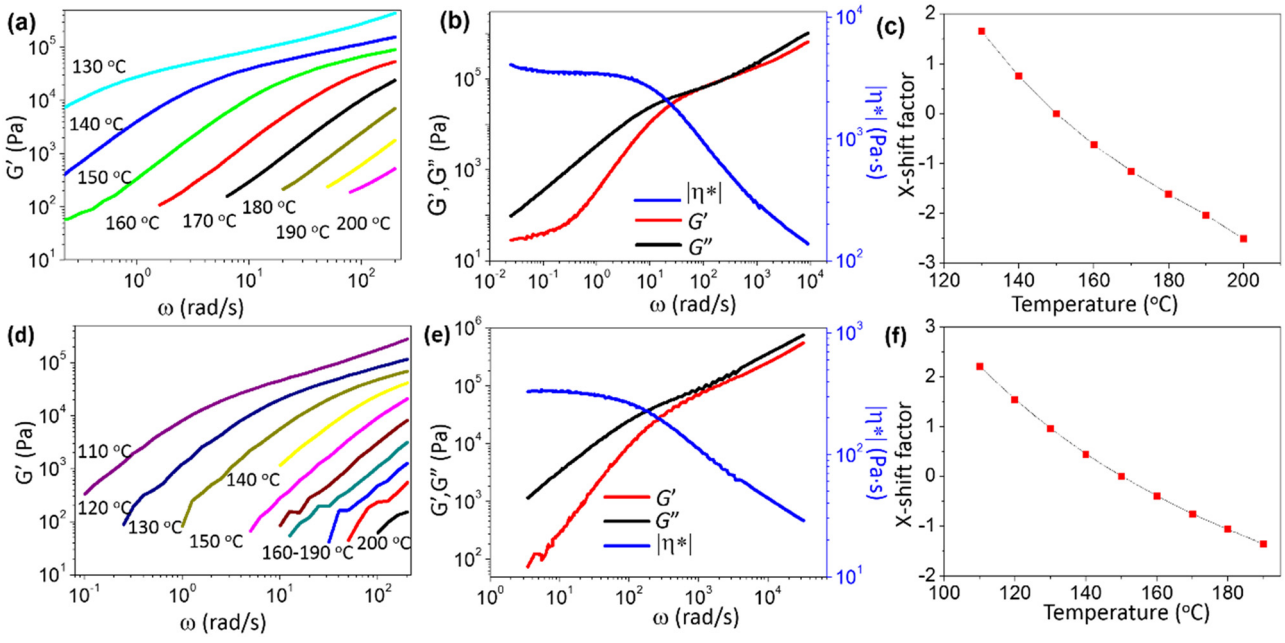

Figure A2: (a) Storage modulus (G') versus angular frequency (ω) at temperature from 130°C to 200°C for (**S***15.4*)$_3$, (b) the master curve at the reference temperature of 150°C for (**S***15.4*)$_3$, (c) the X-shift factor versus temperature for (**S***15.4*)$_3$, (d) storage modulus (G') versus angular frequency (ω) at temperature from 110°C to 200°C for (**S***15.4-0.94*-**B***1.4*)$_3$, (e) the master curve at the reference temperature of 150°C for (**S***15.4-0.94*-**B***1.4*)$_3$, and (f) the X-shift factor versus temperature for (**S***15.4-0.94*-**B***1.4*)$_3$.

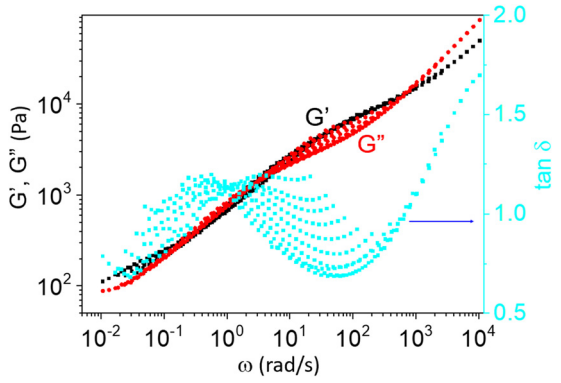

Figure A3: Master curve of (**S***15.4-0.48*-**B***16.7*)$_3$ with *G′*, *G″*, and tan *δ* versus angular frequency (*ω*) with the reference temperature at 150°C.

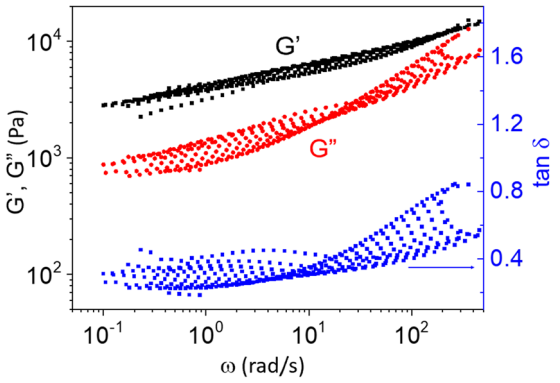

Figure A5: Master curve of (**S***15.4-0.21*-**B***46.6*)$_3$ with *G′*, *G″*, and tan *δ* versus angular frequency (*ω*) with the reference temperature at 150°C.

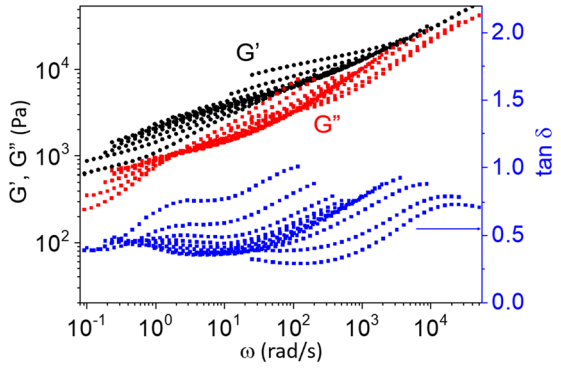

Figure A4: Master curve of (**S***15.4-0.28*-**B***34.3*)$_3$ with *G′*, *G″*, and tan *δ* versus angular frequency (*ω*) with the reference temperature at 150°C.

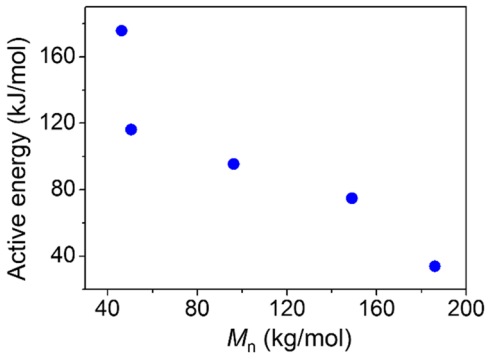

Figure A6: Active energy as a function of M_n of (PS-*b*-PBA)$_3$ at 150°C.